Proceedings of the ASME 2023
International Design Engineering Technical Conferences and
Computers and Information in Engineering Conference
IDETC-CIE2023
August 20-23, 2023, Boston, Massachusetts

DETC2023-116658

CURVATURE ANALYSIS OF LINEAR AND CIRCULAR TRACTRICES FOR THE PLANAR MOTION OF VEHICLES

Chiara Lanni
University of Cassino & Southern Lazio
Dept. of Civil & Mech. Engineering
Cassino (Fr), Italy

Giorgio Figliolini
University of Cassino & Southern Lazio
Dept. of Civil & Mech. Engineering
Cassino (Fr), Italy

Jorge Angeles
McGill University
Dept. of Mech. Engineering & CIM
Montreal (QC), Canada

ABSTRACT

The curvature analysis of the linear and circular tractrix curves for the planar motion of vehicles is formulated as based on the application of the classical differential geometry, along with the Bresse and return circles. In particular, a two-wheel (bicycle) model of four wheels vehicles was assumed and the evolutes of the corresponding fixed centrodes, being the related moving centrodes represented by straight lines, are determined, along with the evolutes of the linear and circular tractrix curves.

The proposed formulation has been implemented in Matlab, in order to simulate and analyze the vehicle behavior in terms of curvature, when the front wheel center follows a straight line or a circle. Significant numerical and graphical results allowed the validation of the proposed formulation in different conditions.

Keywords: Vehicle kinematics, bicycle model, curvature analysis, Bresse's circles, tractrices.

1. INTRODUCTION

The manoeuvring of vehicles riding on wheels, such as cars, buses and trucks, during parking, the changing of lanes when overtaking obstacles and other vehicles, entering into roundabouts, as well as maneuvering upon leaving, are of great interest not only for the safety of bicycles, motorcycles and pedestrians, but also for the design of safe roads and highways [1-4]. In particular, assuming a bicycle model, the path of the rear wheel is a tractrix or equi-tangential curve, which is different from that traced by the front wheel that plays the role of directrix.

One of the earliest examples of an "inverse tangent problem" and determination of a curve by the process of integration, was proposed by Claude Perrault during a meeting that was held in Paris in 1693, as reported in [5-6]. However, the equation of this curve has already been derived by Newton in 1676 and studied later by mathematicians of calibre of Leibniz, Huygens and Euler. The name "tractrix", from Latin "tractus", to pull, was given by Huygens, but a reverse tractrix can be also drawn by pushing a drawbar. The linear tractrix can also be generated as the involute of a catenary, which was discovered by Jakob Bernoulli in 1691. In addition to the linear tractrix, a circular tractrix can be drawn, when the directrix is a circle, the corresponding method can be further extended to a general tractrix, referring to a generic planar curve. The geometric properties of the tractrix and catenary, as transcendental curves, have been analyzed and discussed in several geometry book [7-11]. However, the curvature analysis of linear and circular tractrices for the planar motion of four wheels vehicles, which are sketched by using the bicycle model, is proposed here for the first time, as based on the fundamentals of the kinematics of planar mechanisms, while extending the previous results reported in [12] and [13].

In fact, in this paper the focus is the curvature analysis of the linear and circular tractrices, which has been developed by using the moving and the fixed centrodes and determining the evolute of the fixed centrode, along with the inflection and cuspidal circles. Fundamentals on centrodes and geometric loci can be found in [14-18], along with several applications in [19-22].

In particular, the curvature analysis of the linear and circular tractrix curves for the planar motion of vehicles is formulated as based on the application of the classical differential geometry, along with the Bresse and return circles. A two-wheel (bicycle) model of four wheels vehicles was assumed and the evolutes of the corresponding fixed centrodes, being the related moving centrodes represented by straight lines, are determined, along with the evolutes of the linear and circular tractrix curves.

The proposed formulation has been implemented in Matlab, in order to simulate and analyze the vehicle behavior in terms of curvature, when the front wheel center follows a straight line or a circle. Significant numerical and graphical results allowed the validation of the proposed formulation in different conditions.

2. CURVATURE ANALYSIS: LINEAR TRACTRIX

The linear tractrix is the trajectory of the rear wheel center of a bicycle model, while the front wheel center traces a straight line. The vehicle chassis is sketched through a rigid link that connects both wheel centers, which is known as the drawbar. Assuming as starting configuration of the vehicle that for which the projected lines of the front and back wheels lie at right angles, the linear tractrix shows a cusp at the rear wheel center and an asymptote coinciding with the straight path.

Referring to Fig. 1, an arbitrary configuration AB of the drawbar is shown, while the front and rear wheel centers, A and B, trace the straight path and the linear tractrix curve (dashed line), respectively. The starting configuration of the bicycle vehicle model is A_0B_0 and the drawbar remains tangent to the tractrix curve during the planar motion.

The equation of the linear tractrix can be obtained in Cartesian form by assuming a drawbar of length a and the reference frame OXY, the origin O coinciding with A_0 and the Y-axis oriented along the straight path. In particular, one has

$$y = a\log\left(\frac{a+\sqrt{a^2-x^2}}{x}\right)-\sqrt{a^2-x^2} \qquad 0 \le x \le a \qquad (1)$$

where the Y-axis is the directrix.

Referring to Fig. 1, when the front wheel center A moves along the Y-axis and consequently, the rear wheel center B traces the linear tractrix, the instant center of rotation I coincides with the center of curvature Ω of the tractrix curve and the drawbar AB is always oriented along its tangent line. This means that the moving centrode l is a line identical to the rear wheel axis, while the fixed centrode λ coincides with the tractrix evolute, since representing also the locus of its centers of curvature.

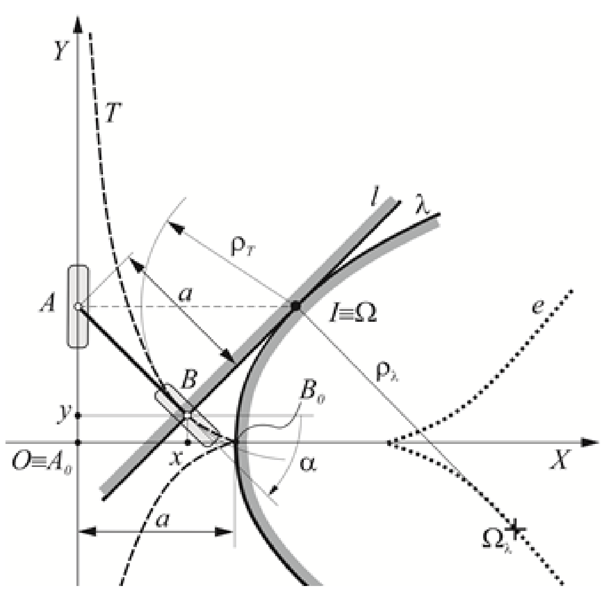

FIGURE 1: LINEAR TRACTRIX T, MOVING l AND FIXED λ CENTRODES, ALONG WITH THE EVOLUTE e OF λ.

The equation of the fixed centrode λ can be obtained as the trajectory of the instant center of rotation I, which can be found, in turn, as the intersection between the normals to the paths of points A and B, according to the Chasles theorem.

The locus of the centers of curvature is called the evolute of the curve, whereas the original curve is the involute of the new one. The tangent to the evolute is the normal to the tractrix (involute), its length ρ_T, measured between the two curves, being the radius of curvature of the tractrix. In the case of Fig. 1, the tractrix is an involute of the fixed centrode λ and the fixed centrode λ is the evolute of the tractrix.

The radius of curvature ρ_T of the linear tractrix of Eq. (1) is

$$\rho_T = \frac{a\sqrt{a^2-x^2}}{x}. \qquad (2)$$

and its evolute takes the form

$$y_\Omega = a\log\left(\frac{x_\Omega+\sqrt{x_\Omega^2-a^2}}{a}\right) \qquad (3)$$

which is a catenary, whose vertex is at point B_0 (a, 0).

Moreover, the tangent to the evolute e of the catenary (fixed centrode λ) that plays the role of its involute, coincides with the normal to the catenary of radius of curvature ρ_λ and center of curvature Ω_λ. The evolute of the catenary is given by

$$y_e = -\frac{x_e}{4a}\sqrt{x_e{}^2-4a^2}+a\log\left(\frac{x_e+\sqrt{x_e{}^2-4a^2}}{2a}\right) \qquad (4)$$

where x_e and y_e correspond to the coordinates of Ω_λ and a is length of the drawbar AB.

In order to develop the curvature analysis of the linear tractrix for the planar motion of vehicles that are sketched through a bicycle model, the inflection and return circles are determined.

These loci are tangent to each other and to the fixed and moving centrodes at the instant center of rotation, during their pure rolling motion. In particular, the inflection circle $\mathcal{I}$ is the instantaneous locus of all points of the moving plane, showing an inflection point in their trajectories, while the return circle $\mathcal{R}$, the mirror image of the inflection circle, is the locus of the centers of curvature of all moving points at infinity.

Thus, referring to Fig. 2 and applying the Euler-Savary equation, one has that $\rho_\lambda = -\Delta$ where the moving centrode is a straight line ($\rho_l \to \infty$) and Δ is the diameter of both circles $\mathcal{I}$ and $\mathcal{R}$, which are tangent to the centrodes at the instant center of rotation I, where W and R are the inflection and cuspidal poles. The inflection circle $\mathcal{I}$ includes the front wheel center A of the drawbar AB, since it moves along a straight line (Y-axis). In particular, each circle has been expressed in vector form through a position vector, as reported in [12].

A significant property of a family of the catenary curves, which are also the fixed centrodes of the drawbar *AB* planar motion and, at the same time, the evolutes of the corresponding tractrix curves, is that they envelope a straight line passing through the origin *O* of the fixed frame *OXY* of Fig. 1.

This property can be proven by considering the family of the catenary as a function of the parameter *a*, namely,

$$F\left(x_{\Omega}, y_{\Omega}, a\right)=\frac{y_{\Omega}}{a}-\log\left(\frac{x_{\Omega}+\sqrt{x_{\Omega}^{2}-a^{2}}}{a}\right)=0 \tag{5}$$

and imposing the tangency condition between each curve of the family and the envelope curve:

$$\frac{\partial}{\partial a}F\left(x_{\Omega}, y_{\Omega}, a\right)=0 \tag{6}$$

Thus, Eq. (6) leads to the expression of the parameter *a*, i.e.,

$$a=\sqrt{\frac{x_{\Omega}^{2}y_{\Omega}^{2}}{x_{\Omega}^{2}+y_{\Omega}^{2}}} \tag{7}$$

which is substituted into Eq. (5) to give the envelope curve as

$$\frac{\sqrt{x_{\Omega}^{2}+y_{\Omega}^{2}}}{x_{\Omega}}-\log\left(\frac{x_{\Omega}+\sqrt{x_{\Omega}^{2}+y_{\Omega}^{2}}}{y_{\Omega}}\right)=0 \tag{8}$$

This is the equation of a straight line passing through the origin *O* of *OXY* and tangent to each catenary of the family.

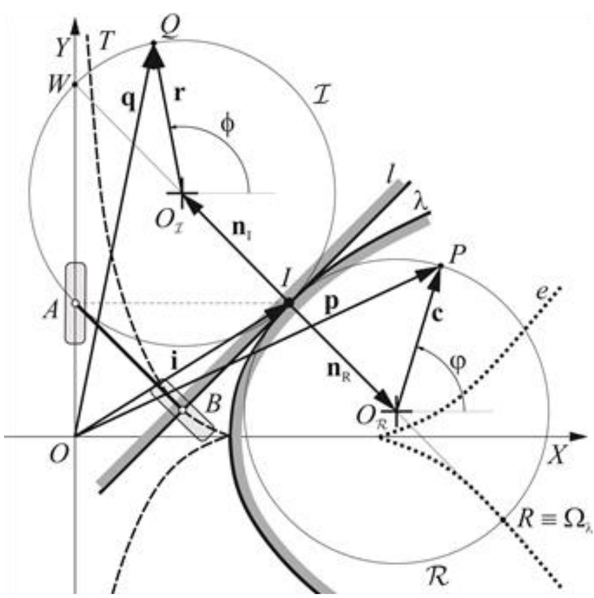

FIGURE 2. CURVATURE ANALYSIS: INFLECTION $\mathcal{I}$ AND RETURN $\mathcal{R}$ CIRCLES.

3. LINEAR TRACTRIX: RESULTS

The first part of the proposed formulation, based on the Eqs. (1) to (8), was implemented in Matlab, to produce the graphical and numerical results shown in Figs. 3 and 4. In particular, Fig. 3a shows the linear tractrix (dashed-line), the fixed λ (catenary) and the moving *l* (straight-line) centrodes, along with the evolute *e* of the catenary. The inflection $\mathcal{I}$ and the return $\mathcal{R}$ circles are also shown for a specific configuration of the drawbar *AB*.

Moreover, as expected, the center of curvature Ω of the catenary coincides with the cuspidal center *R* of the return circle $\mathcal{R}$, while the inflection circle $\mathcal{I}$ passes through the front wheel center *A* and the inflection pole *W*.

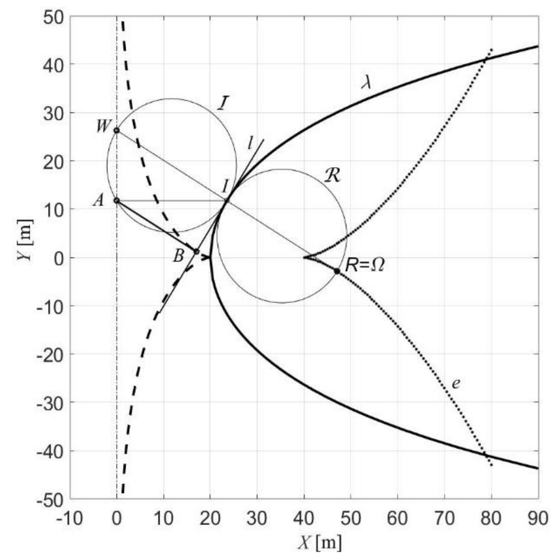

a)

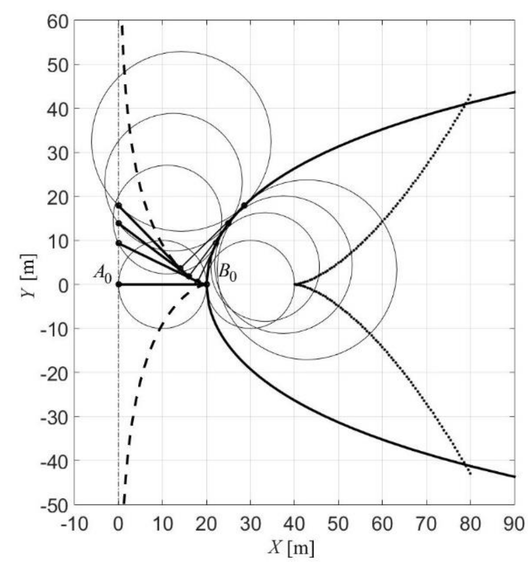

b)

FIGURE 3. LINEAR TRACTRIX: FIXED λ AND MOVING *l* CENTRODES, EVOLUTE *e* OF λ, INFLECTION $\mathcal{I}$ AND THE RETURN $\mathcal{R}$ CIRCLES.

Figure 3b illustrates a family of inflection and return circles, whose diameter changes according to the radius of curvature of the catenary at the instant center of rotation for different drawbar configurations. Figure 4a shows some interesting curvature properties of the tractrix curve, which can be useful to foresee the planar motion of the bicycle vehicle model according to the length a of the drawbar AB.

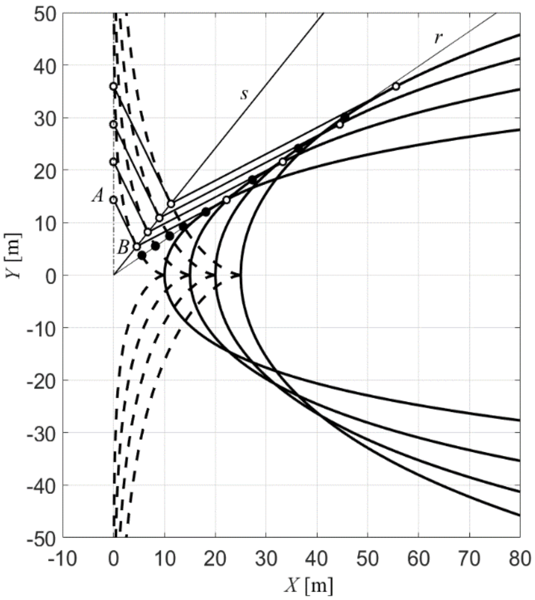

a)

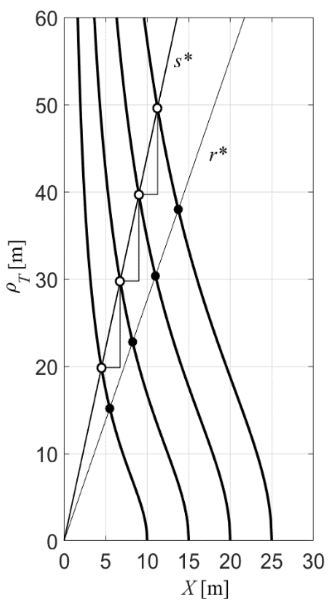

b)

FIGURE 4. CURVATURE PROPERTIES OF THE LINEAR TRACTRIX CURVE: a) FAMILY OF TRACTRIX CURVES (DASHED LINES), ALONG WITH THE FAMILY OF THEIR EVOLUTES (THICK CONTINUOUS LINES); b) DIAGRAM OF THE RADIUS OF CURVATURE ρ_T FOR THE FAMILY OF TRACTRICES.

In fact, increasing a, a family of almost parallel linear tractrix curves (dashed-lines) is generated, along with a related family of catenary curves, as shown in Fig. 4a. Moreover, the envelope of the same family gives the straight line r passing through the origin O of the fixed reference frame OXY, while, for a generic line s passing through O, one has a family of straight lines that are tangent to the correspondent family of catenary curves. Correspondingly, Fig. 4b depicts the variation of the radius of curvature ρ_T of the tractrix curve versus X for different lengths a of the drawbar AB, where the straight lines r^* and s^* correspond to r and s of Fig. 4a, respectively. In particular, a line s passing through the origin O intersects all tractrix curves of the family, one for each length a of the drawbar AB, at points whose corresponding centers of curvature lie on parallel lines that are tangent to their related catenary curves, as shown in Fig. 4a.

Moreover, referring to Fig. 4b, the radii of curvature ρ_T of the family of tractrix curves, as functions of a, change of the same value, while increasing the angular coefficient of the line s^*, the range of variation of the corresponding radius of curvature is constant, but higher. When this line coincides with the envelope line of the family of catenary curves, this property is preserved, but the centers of curvature are also aligned along the same line normal to each tractrix curve.

4. CURVATURE ANALYSIS: CIRCULAR TRACTRICES

Before to develop the curvature analysis and referring to the bicycle kinematic model of Fig. 5 and Fig. 6, which sketches a vehicle chassis that moves in the OXY plane along a circular path, the equations of the inner and outer circular tractrices are here recalled, since obtained previously in [12] and [13].

In particular, the drawbar AB has fixed length a and it represents the vehicle chassis, while r_A indicates the radius of the circle followed by the front wheel center A, $b = \overline{OB}$ the radius of the circle followed by the rear wheel center B, φ denoting the angle swept by A with respect to the X-axis and angle γ defines the angular position of $\mathbf{r}_A$ with respect to $\mathbf{a}$.

In order to describe the path of the rear wheel center B, the position vector $\mathbf{b}$ of point B is obtained as

$$\mathbf{b} = \mathbf{r}_A + \mathbf{a} \tag{9}$$

Moreover, $\mathbf{r}_A$ and $\mathbf{a}$ are expressed in Cartesian form as

$$\mathbf{r}_A = \left[r_A \cos\varphi \quad r_A \sin\varphi \right]^T \tag{10}$$

$$\mathbf{a} = \left[a\cos(\varphi-\gamma) \quad a\sin(\varphi-\gamma) \right]^T \tag{11}$$

where r_A is the radius of the circular path of A.

Thus, according to what obtained in [?] and [?], one has

$$\varphi_{(\gamma)} = \frac{a}{b} \log \left| \frac{(r_A - a)\tan\frac{\gamma}{2} + b}{(r_A - a)\tan\frac{\gamma}{2} - b} \right| \tag{12}$$

where $b=\sqrt{{r_A}^2-a^2}$ is the magnitude of vector **b** and $r_A > a$.

Solving Eq. (12) for γ, two solutions can be obtained because of the absolute value of the logarithmic function argument. These two solutions represent specific cases of the circular tractrix, the inner and the outer cases, namely,

$$\gamma_{(\varphi)}=2\,\mathrm{atan}\left(s\,\frac{\mathrm{e}^{k\varphi}+1}{\mathrm{e}^{k\varphi}-1}\right),\qquad \gamma_{(\varphi)}=2\,\mathrm{atan}\left(s\,\frac{\mathrm{e}^{k\varphi}-1}{\mathrm{e}^{k\varphi}+1}\right) \tag{13}$$

where $k=b/a$ and $s=b/(r_A-a)$.

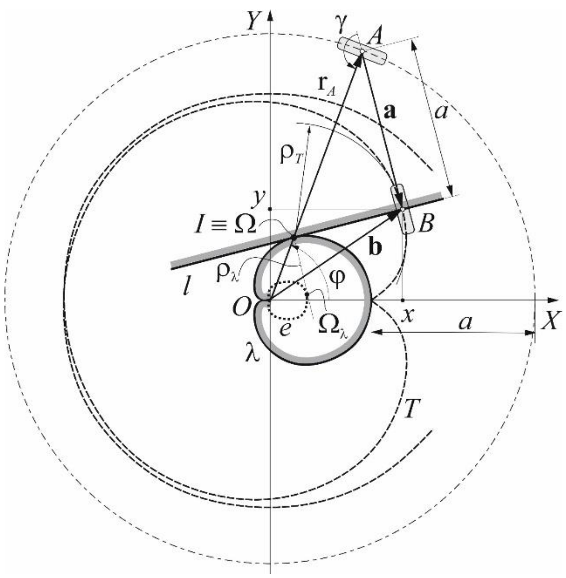

FIGURE 5. INNER CIRCULAR TRACTRIX, ALONG WITH THE FIXED λ AND MOVING l CENTRODES.

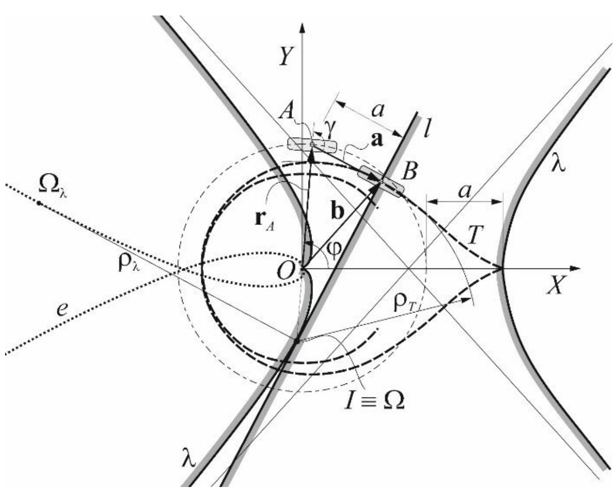

FIGURE 6. OUTER CIRCULAR TRACTRIX, ALONG WITH THE FIXED λ AND THE MOVING l CENTRODES.

In particular, the first of Eqs. (13) gives the inner tractrix of Fig. 5, whereby the curve lies inside the circle of radius r_A, since it is traced by the rear wheel center B, while the front wheel center A follows the circular path. Similarly, the second of Eqs. (13) gives the outer tractrix of Fig. 6, in which a branch of the curve lies inside the circle of radius r_A, the other branch lying outside. At the starting configuration, the drawbar AB of length a is assumed aligned with the X-axis and having its front wheel center A moving along the circle of radius r_A. The difference between the inner and the outer circular tractrix curves is the starting position of the rear wheel center B, which is located inside the circle for the case of Fig. 5 and outside for that of Fig.6.

Still referring to the sketch of Fig. 5, in general, the planar motion of the chassis of the vehicle can be represented by means of the *fixed* and *moving centrodes*, which are in contact at the instant center of rotation I on the ground (fixed centrode) and on the moving plane AB that is attached to the vehicle (moving centrode), respectively. The path normal to the traction curve maintains a constant angle with the drawbar of length a, all instant centers lying on the same line of the drawbar. This means that the moving centrode is a line l normal to the rear wheel axis and, consequently, the fixed centrode coincides with the evolute of the circular tractrix, which can also be obtained as its involute.

The circular tractrix is an involute of the fixed centrode λ, while the fixed centrode λ is the evolute of the tractrix. The tangent to the evolute is the normal to the circular tractrix (involute); its length ρ_T, measured between the two curves, is the radius of curvature of the circular tractrix (involute).

The radius of curvature ρ of a curve can be expressed as

$$\rho=\frac{\sqrt{\left(x'^2+y'^2\right)^3}}{x'\,y''-y'\,x''} \tag{14}$$

the first and second derivatives being taken w.r.t. the parameter in question; in our case the parameter is angle φ, the partial derivatives being

$$\begin{aligned} x' &= -r_A\sin\varphi - a\left(1-\gamma'\right)\sin\left(\varphi-\gamma\right)\\ y' &= r_A\cos\varphi + a\left(1-\gamma'\right)\cos\left(\varphi-\gamma\right) \end{aligned} \tag{15}$$

$$\begin{aligned} x'' &= -r_A\cos\varphi - a\left[\left(-\gamma''\right)\sin\left(\varphi-\gamma\right)+\left(1-\gamma'\right)^2\cos\left(\varphi-\gamma\right)\right]\\ y'' &= -r_A\sin\varphi + a\left[\left(-\gamma''\right)\cos\left(\varphi-\gamma\right)-\left(1-\gamma'\right)^2\sin\left(\varphi-\gamma\right)\right] \end{aligned} \tag{16}$$

The first and second derivatives of angle γ, are given by

$$\gamma' = -\frac{4\,s\,k\,\mathrm{e}^{k\varphi}}{s^2\left(\mathrm{e}^{k\varphi}+1\right)^2+\left(\mathrm{e}^{k\varphi}-1\right)^2} \tag{17}$$

$$\gamma'' = \frac{4\cdot s\cdot k^2\cdot\left(1+s^2\right)\cdot\mathrm{e}^{k\varphi}\left(\mathrm{e}^{2k\varphi}-1\right)}{\left[s^2\left(\mathrm{e}^{k\varphi}+1\right)^2+\left(\mathrm{e}^{k\varphi}-1\right)^2\right]^2} \tag{18}$$

for the *inner circular tractrix* of Fig. 5, for the *outer circular tractrix* of Fig. 6, in turn, we have

$$\gamma' = \frac{4 \cdot s \cdot k \cdot \mathrm{e}^{k\varphi}}{s^2\left(\mathrm{e}^{k\varphi}-1\right)^2+\left(\mathrm{e}^{k\varphi}+1\right)^2} \tag{19}$$

$$\gamma'' = -\frac{4\, s\, k^2\left(1+s^2\right)\mathrm{e}^{k\varphi}\left(\mathrm{e}^{2k\varphi}-1\right)}{\left[s^2\left(\mathrm{e}^{k\varphi}-1\right)^2+\left(\mathrm{e}^{k\varphi}+1\right)^2\right]^2} \tag{20}$$

The locus of the center of curvature Ω of the circular tractrix is the evolute of the curve; the circular tractrix can be generated as its involute. The evolute λ of the circular tractrix represents also the fixed centrode of the planar drawbar motion since the moving centrode l coincides with the straight line normal to the drawbar AB at the rear wheel center B. Thus, the equation of λ can be readily obtained in parametric form as

$$x_\lambda = x - y'\frac{x'^2+y'^2}{x'y''-y'x''} = x - y' H \tag{21}$$

$$y_\lambda = y + x'\frac{x'^2+y'^2}{x'y''-y'x''} = y + x' H \tag{22}$$

Similarly, the second order evolute e of the circular tractrix is given by

$$x_e = x_\lambda - y_\lambda'\frac{x_\lambda'^2+y_\lambda'^2}{x_\lambda' y_\lambda''-y_\lambda' x_\lambda''} \tag{23}$$

$$y_e = y_\lambda + x_\lambda'\frac{x_\lambda'^2+y_\lambda'^2}{x_\lambda' y_\lambda''-y_\lambda' x_\lambda''}\,. \tag{24}$$

where x_e and y_e are the Cartesian coordinates of the center of curvature Ω_λ of the first evolute λ of the tractrix, while ρ_e is the corresponding radius of curvature that can be obtained upon replacing Eqs. (28) and (29), and either Eq. (30) or Eq. (31), into Eq. (27), for the inner and the outer circular tractrix curves, respectively. Thus, the first and second derivatives of Eqs. (21) and (22) can be expressed as

$$\begin{aligned} x_\lambda' &= x' - \left(y''H + y'H'\right) \\ y_\lambda' &= y' + x''H + x'H' \end{aligned} \tag{25}$$

$$\begin{aligned} x_\lambda'' &= x'' - \left(y'''H + 2y''H' + y'H''\right) \\ y_\lambda'' &= y'' + x'''H + 2x''H' + x'H'' \end{aligned} \tag{26}$$

where

$$H' = \frac{2\left(x'x''+y'y''\right)\left(x'y''-y'x''\right)}{\left(x'y''-y'x''\right)^2} + -\frac{\left(x'^2+y'^2\right)\left(x'y'''-y'x'''\right)}{\left(x'y''-y'x''\right)^2} \tag{27}$$

$$\begin{aligned} H'' = {}& \frac{2\left(x''^2+x'x'''+y''^2+y'y'''\right)\left(x'y''-y'x''\right)\left(x'y''-y'x''\right)}{\left(x'y''-y'x''\right)^3} + \\ & -\frac{\left(x'^2+y'^2\right)\left(x''y'''+x'y^{\mathrm{iv}}-y''x'''-y'x^{\mathrm{iv}}\right)\left(x'y''-y'x''\right)}{\left(x'y''-y'x''\right)^3} + \\ & -\frac{2\left(x'x''+y'y''\right)\left(x'y''-y'x''\right)\left(x'y'''-y'x'''\right)}{\left(x'y''-y'x''\right)^3} + \\ & +\frac{2\left(x'^2+y'^2\right)\left(x'y'''-y'x'''\right)\left(x'y'''-y'x'''\right)}{\left(x'y''-y'x''\right)^3} \end{aligned} \tag{28}$$

and

$$\begin{aligned} x''' &= r_A\sin\varphi + a\left[\gamma''' + \left(1-\gamma'\right)^3\right]\sin\left(\varphi-\gamma\right) + \\ &\quad + 3a\left(1-\gamma'\right)\gamma''\cos\left(\varphi-\gamma\right) \\ y''' &= -r_A\cos\varphi - a\left[\gamma''' + \left(1-\gamma'\right)^3\right]\cos\left(\varphi-\gamma\right) + \\ &\quad + 3a\left(1-\gamma'\right)\gamma''\sin\left(\varphi-\gamma\right) \end{aligned} \tag{29}$$

$$\begin{aligned} x^{\mathrm{iv}} &= r_A\cos\varphi + a\left[\gamma^{\mathrm{iv}} - 6\gamma''\left(1-\gamma'\right)^2\right]\sin\left(\varphi-\gamma\right) + \\ &\quad + \left[a\left(1-\gamma'\right)^4 - 3\gamma''^2 + 4\left(1-\gamma'\right)\gamma'''\right]\cos\left(\varphi-\gamma\right) \\ y^{\mathrm{iv}} &= r_A\sin\varphi + a\left[\gamma^{\mathrm{iv}} + 6\gamma''\left(1-\gamma'\right)^2\right]\cos\left(\varphi-\gamma\right) + \\ &\quad + \left[a\left(1-\gamma'\right)^4 - 3\gamma''^2 + 4\left(1-\gamma'\right)\gamma'''\right]\sin\left(\varphi-\gamma\right) \end{aligned} \tag{30}$$

Thus, the third and fourth derivatives of $\gamma_{(\varphi)}$ as expressed by the first of Eq. (26) for the inner tractrix, are displayed below

$$\begin{aligned} \gamma''' = {}& \frac{4sk^3\left(1+s^2\right)\mathrm{e}^{k\varphi}}{\left[s^2\left(\mathrm{e}^{k\varphi}+1\right)^2+\left(\mathrm{e}^{k\varphi}-1\right)^2\right]^3}\Big[\left(s^2+1\right)\cdot \\ & \cdot\left(-\mathrm{e}^{4k\varphi}+6\mathrm{e}^{2k\varphi}-1\right)+2\left(s^2-1\right)\left(\mathrm{e}^{3k\varphi}+\mathrm{e}^{k\varphi}\right)\Big] \end{aligned} \tag{31}$$

$$\begin{aligned} \gamma^{\mathrm{iv}} = {}& \frac{4sk^4\left(1+s^2\right)\mathrm{e}^{k\varphi}}{\left[s^2\left(\mathrm{e}^{k\varphi}+1\right)^2+\left(\mathrm{e}^{k\varphi}-1\right)^2\right]^4}\Big\{\Big[\left(s^2+1\right)\cdot \\ & \cdot\left(18\mathrm{e}^{2k\varphi}-5\mathrm{e}^{4k\varphi}-1\right)+4\left(s^2-1\right)\left(2\mathrm{e}^{3k\varphi}+\mathrm{e}^{k\varphi}\right)\Big]\cdot \\ & \cdot\left[s^2\left(\mathrm{e}^{k\varphi}+1\right)^2+\left(\mathrm{e}^{k\varphi}-1\right)^2\right]-6\mathrm{e}^{k\varphi}\Big[\left(s^2+1\right)\cdot \\ & \cdot\left(-\mathrm{e}^{4k\varphi}+6\mathrm{e}^{2k\varphi}+\mathrm{e}^{k\varphi}-1\right)+\left(s^2-1\right)\left(2\mathrm{e}^{3k\varphi}+\mathrm{e}^{k\varphi}+1\right)\Big]\Big\} \end{aligned} \tag{32}$$

Similarly, the third and fourth derivatives of $\gamma_{(\varphi)}$ as expressed by the second of Eq. (26) for the outer tractrix, are given by

$$\gamma''' = -\frac{4sk^3\left(1+s^2\right)e^{k\varphi}}{\left[s^2\left(e^{k\varphi}-1\right)^2+\left(e^{k\varphi}+1\right)^2\right]^3}\Big[\left(s^2+1\right)\bullet$$
$$\bullet\left(-e^{4k\varphi}+6e^{2k\varphi}-1\right)+2\left(1-s^2\right)\left(e^{3k\varphi}+e^{k\varphi}\right)\Big] \qquad (33)$$

$$\gamma^{\text{iv}} = -\frac{4sk^4\left(1+s^2\right)e^{k\varphi}}{\left[s^2\left(e^{k\varphi}-1\right)^2+\left(e^{k\varphi}+1\right)^2\right]^4}\Big\{\Big[\left(s^2+1\right)\cdot$$
$$\cdot\left(18e^{2k\varphi}-5e^{4k\varphi}-1\right)+4\left(1-s^2\right)\left(2e^{3k\varphi}+e^{k\varphi}\right)\Big]\cdot \qquad (34)$$
$$\cdot\left[s^2\left(e^{k\varphi}-1\right)^2+\left(e^{k\varphi}+1\right)^2\right]-6e^{k\varphi}\Big[\left(s^2+1\right)\cdot$$
$$\cdot\left(-e^{4k\varphi}+6e^{2k\varphi}+e^{k\varphi}-1\right)+\left(1-s^2\right)\left(2e^{3k\varphi}+e^{k\varphi}+1\right)\Big]\Big\}$$

5. INFLECTION AND RETURN CIRCLES

As described above, the moving centrode l is represented by the axis of the rear wheel center B and, consequently, the fixed centrode λ coincides with the evolute of the circular tractrix. In particular, the moving centrode lies inside the inner circular tractrix of Fig. 5, while the moving centrode is composed by two branches in the case of the outer circular tractrix of Fig. 6, because the drawbar AB of the bicycle vehicle model is located along the X-axis and outside the circular path of the front wheel center A, at the starting configuration. Referring to Fig. 7, the *inflection circle* $\mathcal{I}$ is tangent to l at the instant center of rotation I and passes through the corresponding inflection point A' of A, whose position in terms of the oriented segment $\overline{A'A}$, can be

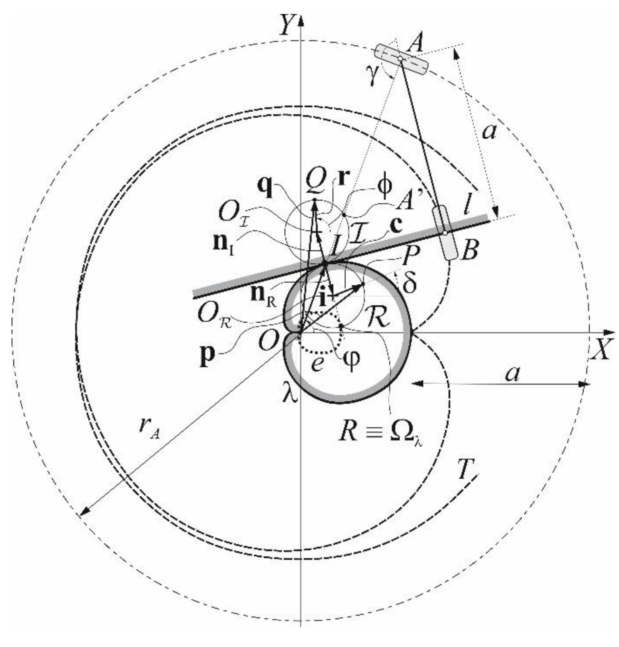

FIGURE 7. INNER CIRCULAR TRACTRIX: FIXED λ AND MOVING L CENTRODES, ALONG WITH THE INFLECTION $\mathcal{I}$ AND THE RETURN $\mathcal{R}$ CIRCLES.

obtained by the Euler-Savary equation as

$$\left(\overline{IA}\right)^2 = \left(\overline{\Omega_\lambda A}\right)\left(\overline{A'A}\right) = r_A\left(\overline{A'A}\right) \qquad (35)$$

$$\overline{A'A} = \frac{\left(\overline{IA}\right)^2}{r_A} = \frac{\left(x_A-x_I\right)^2+\left(y_A-y_I\right)^2}{r_A} \qquad (36)$$

where $\overline{IA}$, $\overline{\Omega_\lambda A}$ and $\overline{A'A}$ are oriented segments, positive from the first to the second point, as from I to A. Since point A moves along the circular path of radius r_A, its center of curvature Ω_A coincides with the origin O and $\overline{\Omega_\lambda A} = r_A$. Moreover, $\overline{IA}$ is expressed as a function of the Cartesian coordinates of points I and A. The radius of curvature ρ_λ of the fixed centrode λ is

$$\rho_\lambda = \frac{IA'}{\cos(\pi-\gamma)} = \frac{\sqrt{\left(x_{A'}-x_I\right)^2+\left(y_{A'}-y_I\right)^2}}{\cos(\pi-\gamma)} \qquad (37)$$

The center of curvature Ω_λ of the fixed centrode λ coincides with the cuspidal pole R, which is opposite to I on the return circle $\mathcal{R}$, and consequently, the radius of curvature of λ at point I is given by the diameter of $\mathcal{R}$, which is equal to that of $\mathcal{I}$.

Referring to Figs. 7 and 8 respectively, the vector function of the *inflection circle* $\mathcal{I}$ is given by the position vector $\mathbf{q}$ of point Q of $\mathcal{I}$, as

$$\mathbf{q} = \mathbf{i} + \mathbf{n}_I + \mathbf{r} \qquad (38)$$

where vectors $\mathbf{i}$, $\mathbf{n}_I$ and $\mathbf{r}$ are given by

$$\mathbf{i} = \left[\cos\varphi\left(r_A+\frac{a}{\cos\gamma}\right) \quad \sin\varphi\left(r_A+\frac{a}{\cos\gamma}\right)\right]^T \qquad (39)$$

$$\mathbf{n}_I = \rho_\lambda\left[\cos(\varphi-\gamma) \quad \sin(\varphi-\gamma)\right]^T \quad \mathbf{r} = \rho_\lambda\left[\cos\phi \quad \sin\phi\right]^T \quad (40)$$

Similarly, the vector function of the *return circle* $\mathcal{R}$ can be expressed through the position vector $\mathbf{p}$ of a point P of $\mathcal{R}$, as

$$\mathbf{p} = \mathbf{i} + \mathbf{n}_R + \mathbf{c} \qquad (41)$$

where $\mathbf{i}$ is obtained by the Eq. (39), while $\mathbf{n}_R$ and $\mathbf{c}$ are given by

$$\mathbf{n}_R = -\rho_\lambda\left[\cos(\varphi-\gamma) \quad \sin(\varphi-\gamma)\right]^T \qquad (42)$$

$$\mathbf{c} = \rho_\lambda\left[\cos\delta \quad \sin\delta\right]^T \qquad (43)$$

ρ_λ being the radius of curvature of the fixed centrode.

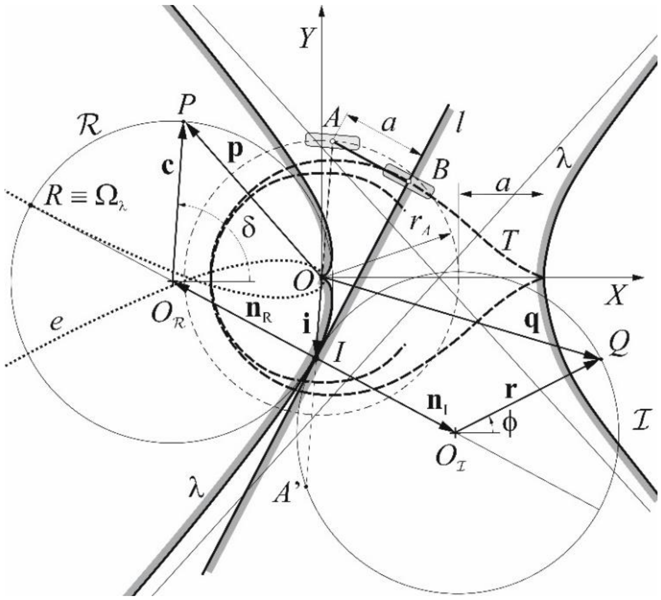

FIGURE 8. OUTER CIRCULAR TRACTRIX: FIXED AND MOVING CENTRODES, ALONG WITH THE INFLECTION $\mathcal{I}$ AND THE RETURN $\mathcal{R}$ CIRCLES.

6. CIRCULAR TRACTRICES: RESULTS

The proposed formulation was implemented in Matlab to produce significant graphical and numerical results, as those shown in Figs. 9 and 10. In particular, Fig. 9a shows the inner circular tractrix (dashed-line), the fixed λ and moving l (straight-line) centrodes, along with the evolute e of λ. Inflection and return circles are also shown for a specific configuration of the drawbar AB. Moreover, as expected, the center of curvature Ω of λ coincides with the cuspidal center R of the return circle $\mathcal{R}$.

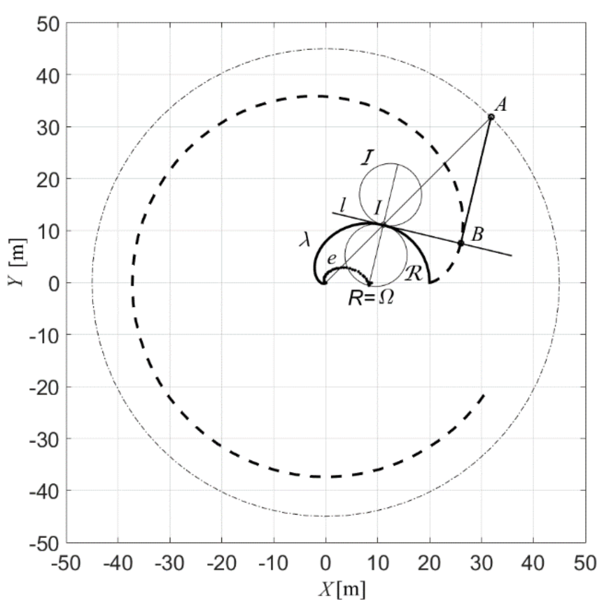

a)

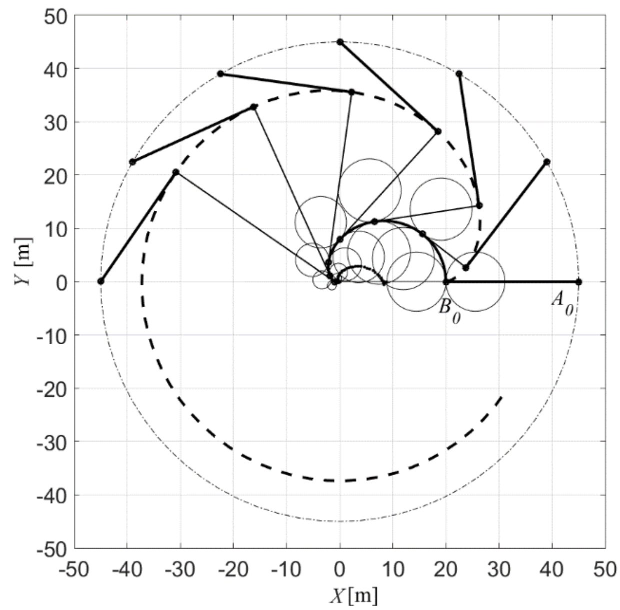

b)

FIGURE 9. INNER CIRCULAR TRACTRIX: FIXED λ AND MOVING l CENTRODES, EVOLUTE e OF λ, INFLECTION $\mathcal{I}$ AND THE RETURN $\mathcal{R}$ CIRCLES.

Figure 9b illustrates a family of inflection and return circles for different drawbar configurations, whose starting position is assumed to be A_0B_0. The diameter of $\mathcal{I}$ and $\mathcal{R}$ changes according to the curvature variation of λ.

Similar to Fig. 9a, Figure 10a shows the outer circular tractrix (dashed-line), the fixed λ and moving l (straight-line) centrodes, along with the evolute e of λ.

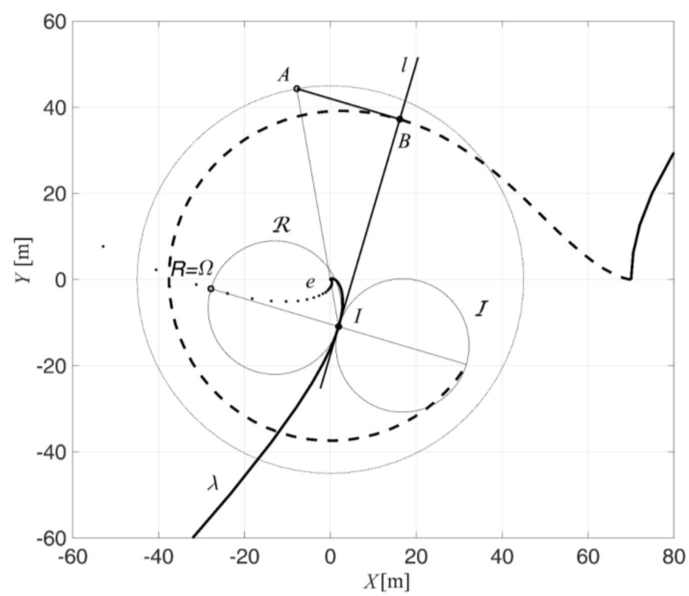

a)

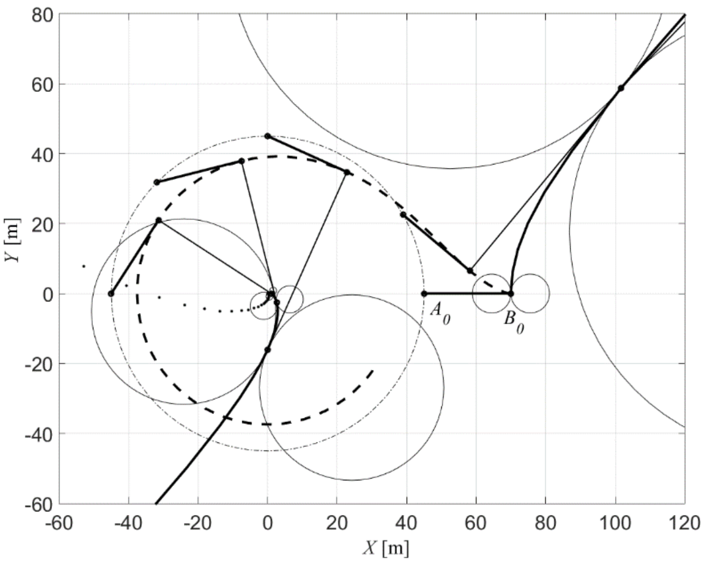

b)

FIGURE 10. OUTER CIRCULAR TRACTRIX: FIXED λ AND MOVING l CENTRODES, EVOLUTE e OF λ, INFLECTION $\mathcal{I}$ AND THE RETURN $\mathcal{R}$ CIRCLES.

The inflection $\mathcal{I}$ and return $\mathcal{R}$ circles are also shown for a specific configuration of the drawbar AB. Of course, the center of curvature Ω of λ coincides with the cuspidal center R of $\mathcal{R}$. As Fig. 9b, Figure 10b illustrates a family of inflection and return circles for different drawbar configurations, whose starting position is A_0B_0.

Figures 11 and 12 show other two examples for a draw-bar length AB = 2.85 m, as the pitch of a common car, and a radius r_A= 5 m. In particular, Fig. 11a and 11b refer to the case of the inner circular tractrix, where the second is a zoom-in of the first.

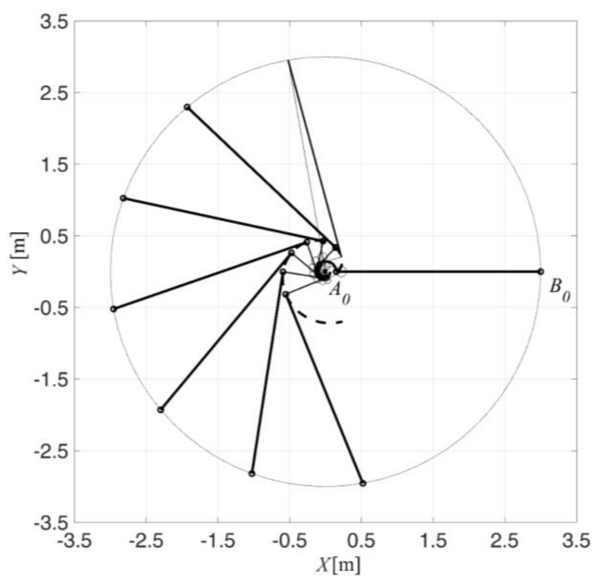

a)

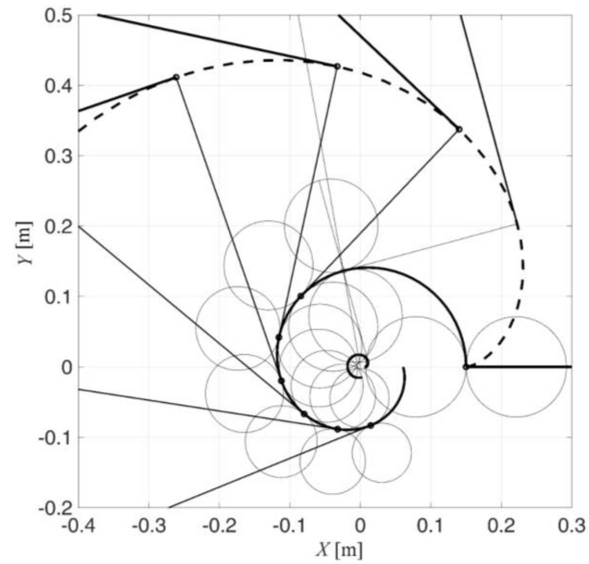

b)

FIGURE 11. INNER CIRCULAR TRACTRIX: a) FIXED λ AND MOVING l CENTRODES, EVOLUTE e OF λ, INFLECTION $\mathcal{I}$ AND THE RETURN $\mathcal{R}$ CIRCLES; b) ZOOM-IN OF FIG. 11a.

Figure 11b shows a family of the inflection and return circles, which are tangent on the opposite sides, to the fixed centrode that is also the evolute of the tractrix. Moreover, the evolute of the fixed centrode is also represented. Figure 12 shows the case of the outer circular tractrix, where both centrodes, the evolute of the fixed centrode, along with the inflection and the return circles are represented. Therefore, the proposed algorithm has been validated for different conditions and dimensions.

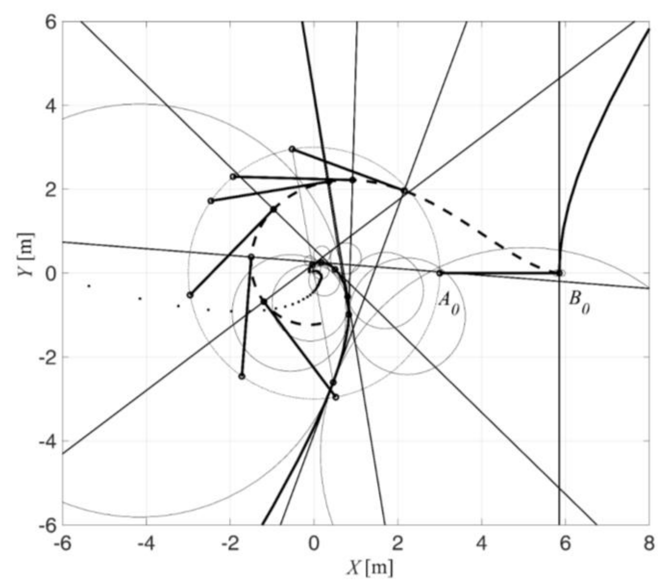

FIGURE 12. OUTER CIRCULAR TRACTRIX: FIXED λ AND MOVING l CENTRODES, EVOLUTE e OF λ, INFLECTION $\mathcal{I}$ AND THE RETURN $\mathcal{R}$ CIRCLES.

7. CONCLUSIONS

The curvature analysis of the linear and circular tractrix curves for the planar motion of vehicles has been formulated as based on the application of the classical differential geometry, along with the Bresse and return circles.

In particular, a two-wheel (bicycle) model of four wheels vehicles was assumed and the evolutes of the corresponding fixed centrodes, being the related moving centrodes represented by straight lines, are determined, along with the evolutes of the linear and circular tractrix curves.

The proposed formulation has been implemented in Matlab, and validated by means of several numerical examples regarding both, the linear and circular tractrices, which have given significant numerical and graphical results.

The bicycle model and the proposed results can be further extended to four wheel vehicles, by considering a rectangular shape of the vehicle chassis that is attached to the draw-bar during its planar motion. The envelop of this rectangular shape will give the vehicle footprint when travelling along tractrix curves and this is very useful in several practical applications, along with the centrodes, Bresse's circles and their evolutes.

ACKNOWLEDGEMENTS

This study was carried out within the MOST – Sustainable Mobility Center and received funding from the European Union Next-Generation EU (PIANO NAZIONALE DI RIPRESA E RESILIENZA (PNRR) – MISSIONE 4 COMPONENTE 2, INVESTIMENTO 1.4 – D.D. 1033 17/06/2022, CN00000023). This manuscript reflects only the authors' views and opinions, neither the European Union nor the European Commission can be considered responsible for them.

REFERENCES

[1] Alexander, J.C., and Maddocks, J. H., 1988, "On the Maneuvering of Vehicles", SIAM Journal on Applied Mathematics, **48** (1), pp. 38–51.

[2] Baylis, J., 1973, "The Mathematics of a Driving Hazard", The Mathematical Gazette, **57** (399), pp. 23–26.

[3] Prince, G.E., and Dubois S.P., 2009, "Mathematical Models for Motion of the Rear Ends Vehicles", Math. and Computer Modelling, **49**, pp. 2049–2060.

[4] Freedman, H.I., and Riemenschneider, S.D., 1983, "Determining the Path of the Rear Wheels of a Bus", Society for Industrial and Applied Mathematical, **25** (4), pp. 561–567.

[5] Foote, R. L., Levi, M., and Tabachnikov, S., 2012, "Tractrices, Bicycle Tire Tracks, Hatchet Planimeters, and a 100-year-old Conjecture", The American Mathematical Monthly, **120** (3), pp. 1–20.

[6] Cady, W. G., 1965, "The Circular Tractrix", The American Mathematical Monthly, **72** (10), pp. 1065–1071.

[7] Salmon, G., 1879, *A Treatise on the Higher Plane Curves: intended as a sequel to a treatise on conic sections*, 3rd Ed., Hodges, Foster, and Figgis, Dublin, pp. 287–290.

[8] Yates, R.C., 1974, *Curves and Their Properties*, National Council of Teachers of Mathematics, Reston, VA (U.S.A.), pp. 221–224.

[9] Lockwood, E. H., 1961, *A Book of Curves*, Cambridge University Press, Cambridge (U.K.). pp. 119–124.

[10] Loria, G., 1930, *Curve Piane Speciali: algebriche e trascendenti*, Vol. 2, Hoepli, Milano, pp. 213–241.

[11] Yates, R.C, 1959, "The Catenary and the Tractrix", The American Mathematical Monthly, **66** (6), pp.500–505.

[12] Figliolini, G., and Lanni, C., 2015, "Kinematic analysis of the planar motion of vehicles when travelling along tractrix curves", Proc. of the ASME International Design Engineering Technical Conferences & Computers and Information in Engineering Conference, Boston (MA), U.S.A., DETC2015-46924.

[13] Figliolini, G., Lanni, C., and Angeles, J. (2020). "Kinematic analysis of the planar motion of vehicles when traveling along tractrix curves." ASME. J. Mechanisms Robotics. October 2020, 12(5): 054502.

[14] Hain, K., 1967, *Applied Kinematics*, 2nd Ed., McGraw Hill, New York, pp. 70–80.

[15] Hall, A.S. Jr., 1986, *Kinematics and Linkage Design*, Waveland Press. Inc., Prospect Heights, IL (U.S.A.), pp. 65–85.

[16] Di Benedetto, A., and Pennestrì, E., 1993, *Introduzione alla Cinematica dei Meccanismi: Moti infinitesimi*, Vol. 2, Casa Editrice Ambrosiana, Milano, pp. 117–144.

[17] Pennestrì, E., and Cera, M., 2023, *Engineering Kinematics: Curvature theory of plane motion*, Amazon Italia Logistica S.r.l., Turin (TO), Italy.

[18] Angeles, J., and Bai, S., 2022, *Kinematics of Mechanical Systems: Fundamental, analysis and synthesis*, Mathematical Engineering, Springer Internationa Publishing, Cham.

[19] Figliolini, G., Rea, P., Angeles, J., 2006, "The Pure-Rolling Cam-Equivalent of the Geneva Mechanism", Mechanism and Machine Theory, **41** (11), pp. 1320-1335.

[20] Figliolini G., Lanni C., Tomassi L. (2020) Kinematic analysis of slider – crank mechanisms via the Bresse and Jerk's circles. In: Carcaterra A., Paolone A., Graziani G. (eds) Proceedings of XXIV AIMETA Conference 2019. AIMETA 2019. Lecture Notes in Mechanical Engineering. Springer, Cham.

[21] Figliolini G., Lanni C., Tomassi L. (2022), First and second order centrodes of slider-crank mechanisms by using instantaneous invariants, In: Altuzarra O., Kecskeméthy A. (Eds.): 18th International Symposium on Advances in Robot Kinematics, ARK 2022, Springer Proceedings in Advanced Robotics, Volume 24 SPAR, p. 303 - 310, Bilbao, 26 – 30 June 2022.

[22] Figliolini, G., Lanni, C. and Sorli, M. (2022) "Kinematic analysis and centrodes between rotating tool with reciprocating motion and workpiece," *Mechanisms and Machine Science*, pp. 54–60.